

Further Commentary on the Sooty Tern Optimization Algorithm and Tunicate Swarm Algorithm

Ngaiming Kwok

Independent Research

ARTICLE INFO

Keywords:

Bio-/Nature-inspired optimization
Sooty Tern Optimization Algorithm
Tunicate Swarm Algorithm
Zero-bias

Abstract

In the article (Kudela, 2022), experimental demonstrations indicated that two Bio-/Nature-inspired optimization algorithms (BNIOAs)—Sooty Tern Optimization Algorithm (STOA) and Tunicate Swarm Algorithm (TSA)—exhibit a zero-bias, leading to the conclusion that the claims made in the original papers were overstated. In this work, we extend the analysis by investigating the source of this bias from a probabilistic perspective. Our findings suggest that operations involving exponentiation, trigonometric functions, and divisions between random numbers are the primary causes of design flaws. These operations result in probability density distributions with a noticeable shift toward zero. Therefore, the application of these two algorithms should be approached with due caution.

1. Introduction

Bio-/Nature-inspired optimization algorithms (BNIOAs), employing the iterative multi-agent (IMA) approach, have become a vibrant research field in which numerous new algorithms are being proposed regularly. Many of these algorithms are applied to solve optimization problems where derivative-based methods are not applicable.

However, there are also many algorithms that contain fundamental design flaws. One of the primary issues, or even criticisms, is the lack of rigorous theoretical support. This is largely due to the exclusive focus on mimicking the corresponding biological or natural metaphor. Although this approach may replicate the natural process, it does not guarantee that the optimization goal will be achieved. In fact, the choice of metaphor is questionable, as the behavior being mimicked is not necessarily relevant to the intended outcomes. Furthermore, the design of BNIOAs has become routine, with ideas being reused, combined, and reinterpreted in its metaphor-based framework.

Several publications in the literature have addressed the aforementioned detrimental problems. For example, insightful critiques are presented in an influential paper (Sørensen, 2015). Despite these critiques, algorithms with questionable designs continue to be introduced. Another commentary article (Kudela, 2022) also deserves attention. Regrettably, the number of citations it has attracted is orders of magnitude fewer than that of the fallacious algorithms it criticized, the Sooty Tern Optimization Algorithm (STOA) (Dhiman and Kaur, 2019) and Tunicate Swarm Algorithm (TSA) (Kaur et al., 2020) published in *Engineering Applications of Artificial Intelligence*. Therefore, a critical investigation of the root causes of these design flaws is imperative.

The present work is motivated by (Kudela, 2022). In addition to the experimental demonstration presented there, this study further investigates the design flaws—specifically, the zero-bias in STOA and TSA, from a probabilistic perspective. The necessity of maintaining appropriate agent positions according to the uniform distribution (UD) is first asserted from the point of view of random search. The key operations in these two algorithms are reviewed and critically examined. Furthermore, appropriate mathematical reasoning and simulations are provided to illustrate the distortion introduced by the UD, which leads to the zero-bias phenomenon.

2. Necessity of Uniform Distribution

Consider an optimization (without loss of generality, minimization) problem that applies the IMA approach, for example:

$$\min f(\mathbf{x}), \text{ such that } f(\mathbf{x}^*) < f(\mathbf{x}), \quad (1)$$

where the solution space is $\mathbf{x} \in \mathbb{R}^D$ of dimension D . It is also assumed that the search (feasible) region is bounded within a hyper-volume $V_s \in \mathbb{R}^D$. The IMA process can be treated as a sequential process of T iterations that deploy

ORCID(s):

N agents at a time in evaluating the objective function $f(\mathbf{x})$. Under these conditions, the probability of finding the optimum at the t th-iteration is:

$$P(t) = 1 - \left(1 - \frac{V_a}{V_s}\right)^t, \quad (2)$$

where $t = 1, \dots, T$ and $V_a \in \mathbb{R}^D$ is the hyper-volume that agent is deployed. It can be seen from Eq. (2) that the probability of finding the optimum is a saturating function. The probability depends on the ratio V_a/V_s . If this ratio is increased, then the number of iterations required can be decreased. This is achievable if the search region is fully covered. In order to avoid duplicated search, the agent positions should be distributed uniformly, that is, samples are required to be drawn from the UD.

3. Concerned Algorithms

The key computation procedures in the two algorithms, STOA and TSA are recalled here. The design irrationalities are highlighted. In the following, we use the proper optimization vocabulary instead of in the language of the metaphor. The mathematical expressions are typeset with proper conventions, we distinguish scalars and vectors using italics and bold lowercase, respectively.

3.1. Sooty Tern Optimization Algorithm

This algorithm mimics the migration and attacking behaviors of the sooty terns corresponding to exploration and exploitation respectively.

Exploration:

Collision avoidance: The position of the agent that does not collide (collision-free) with others is:

$$\mathbf{x}_{ca}(t+1) = \mathbf{x}_{ca}(t) \left(2 - \frac{2t}{T}\right). \quad (3)$$

Convergence to the best-so-far agent: In this stage, the agents are driven towards the best-so-far agent $\mathbf{x}^*(t)$. That is:

$$\mathbf{x}_{cv}(t+1) = 0.5\mathbf{r} \otimes (\mathbf{x}^*(t) - \mathbf{x}_{cv}(t)), \quad (4)$$

where $\mathbf{r} \sim \mathcal{U}(0, 1)$ with dimensions corresponding to \mathbf{x} and the symbol \otimes denotes the Hamadard multiplication.

Update step-size: The agent position update is given by:

$$\Delta\mathbf{x}(t+1) = \mathbf{x}_{ca}(t+1) + \mathbf{x}_{cv}(t+1). \quad (5)$$

Exploitation: In this phase, agents are driven to follow a spiral trajectory. This is achieved by defining:

$$\begin{aligned} \alpha &= \rho \otimes \sin(\theta), \quad \beta = \rho \otimes \cos(\theta), \quad \gamma = \rho \otimes \theta, \\ \rho &= \exp(-\theta), \quad \theta \sim 2\pi\mathcal{U}(0, 1). \end{aligned} \quad (6)$$

It is important to note that in the original paper, Eq. (9) in (Dhiman and Kaur, 2019), ρ is computed from $\exp(\theta)$. The result would be a large number since $\exp(2\pi) = 535.49$. This would drive the agents out of the search space. In the following, the corrected computation is applied.

The updated agent position is obtained from:

$$\mathbf{x}(t+1) = \mathbf{x}^*(t) \otimes \Delta\mathbf{x}(t+1) \otimes (\alpha + \beta + \gamma). \quad (7)$$

3.2. Tunicate Swarm Algorithm

The TSA algorithm mimics the propulsion and swarm behaviors of tunicates. The design incorporates three primary objectives: (1) avoid conflicts, (2) move towards the position of the best-so-far solution, and (3) remain in the vicinity of the best-so-far solution.

Avoiding Conflicts: A movement factor used to update the agent positions is given by:

$$\mathbf{a} = (\mathbf{r}_1 + \mathbf{r}_2 - 2\mathbf{r}_3) \oslash 4\mathbf{r}_3, \quad (8)$$

where $\mathbf{r}_{1,2,3} \sim \mathcal{U}(0,1)$ are random variables with dimensions corresponding to \mathbf{x} , and the symbol \oslash denotes the Hadamard division.

Movement Towards Best-So-Far: The step size for the movement is defined as:

$$\Delta\mathbf{x}(t) = |\mathbf{x}^*(t) - \mathbf{r}_4 \otimes \mathbf{x}(t)|, \quad (9)$$

where $\mathbf{r}_4 \sim \mathcal{U}(0,1)$.

Remaining Around Best-So-Far: To keep the agents in the vicinity of the best-so-far agent, the current position is adjusted as follows:

$$\mathbf{x}(t) \leftarrow \begin{cases} \mathbf{x}^*(t) + \mathbf{a} \otimes \Delta\mathbf{x}(t), & \text{if } \mathbf{r}_5 \geq 0.5, \\ \mathbf{x}^*(t) - \mathbf{a} \otimes \Delta\mathbf{x}(t), & \text{otherwise.} \end{cases} \quad (10)$$

where $\mathbf{r}_5 \sim \mathcal{U}(0,1)$.

Swarm Behavior: The final agent position, determined by the swarm behavior, is given by:

$$\mathbf{x}(t+1) = \mathbf{x}(t) \oslash (1 + \mathbf{r}_3). \quad (11)$$

4. Design Flaws and Zero-Bias

4.1. Sooty Tern Optimization Algorithm

The STOA process explicitly makes use of trigonometric functions (with a uniformly distributed parameter θ), see Eq. (6). Now consider a random number $\theta \sim \mathcal{U}(0, 2\pi)$. Its probability density function (PDF) is $f_\Theta(\theta) = 1/2\pi$. To find the PDF of $y = \sin(\theta)$, we transform the variable so that:

$$f_Y(y) = \sum_i \frac{f_\Theta(\theta_i)}{|dy/d\theta|}, \quad (12)$$

and the sum is over all possible θ values such that $y = \sin(\theta)$. There are two solutions for $y \in [-1, +1]$ for $\theta \in [0, 2\pi]$. In the interval $[0, \pi]$, $\theta_1 = \arcsin(y)$ and $\theta_2 = \pi - \arcsin(y)$ for the interval $[\pi, 2\pi]$. Concerning the derivative, we have $|dy/d\theta| = |\cos(\theta)| = \sqrt{1 - y^2}$. The overall PDF for $\theta \in [0, 2\pi]$ then becomes:

$$f_Y(y) = \frac{f_\Theta(\theta_1)}{|\cos(\theta_1)|} + \frac{f_\Theta(\theta_2)}{|\cos(\theta_2)|} = \frac{1}{\pi\sqrt{1 - y^2}}. \quad (13)$$

It can be observed that when $y = \pm 1$, the PDF tends to infinity and is very distorted from a UD. This occurs at $\theta = \pi/2$ and $3\pi/2$ within the interval $[-1, +1]$. A similar procedure would produce the PDF for $y = \cos(\theta)$. However, it should be noted that the peaks would occur at $\theta = 0$ and π .

From Eq. (7), the update process contains merely multiplications. For the step-size in (5), the first term \mathbf{x}_{ca} diminishes over iterations. The second term \mathbf{x}_{cv} would produce a small value due to the product $0.5\mathbf{r} \in [0, 0.5]$ in Eq. (4). Therefore, irrespective of the value of $\mathbf{x}^*(t)$, the overall update would move towards zero with iterations. This property is not desirable while the location of the optimum cannot be known *a priori* to locate at zero.

4.2. Tunicate Swarm Algorithm

In the conflict-avoidance procedure, as described in Eq. (8), the update involves divisions of random numbers. For the denominator, there is a non-zero probability that it may be less than one. In such a case, the quotient exceeds the value of the numerator. Conversely, when the denominator exceeds one, the quotient becomes smaller than the numerator. Furthermore, the PDF of the quotient will be extended to both the lower and upper bounds of the original denominator, deviating from the UD.

In the movement towards the best-so-far solution, as illustrated in Eq. (9), a threshold is set at 0.5. With this setting, the expected value of the modified agent position, $\mathbf{x}(t)$, will be centered around the best-so-far position, $\mathbf{x}^*(t)$.

In the imitation of swarm behavior, as outlined in Eq. (11), division occurs by a shifted random number. Specifically, the denominator, $1 + \mathbf{r}_3$, is greater than one. As a result, the quotient will be smaller than the numerator. In other words, the updated agent position is driven towards zero.

5. Illustrations of the PDF

Simulations are conducted to produce the PDFs of the outcomes from the operations in STOA and TSA. First, we let the existence of the optimum in the search region be unknown. Furthermore, based on the principle of maximum uncertainty, the PDF of the variables follows the UD before being operated. It is also assumed that the variable span includes the origin (at zero) of the search space. To obtain smooth PDFs, 10^6 samples are used, the span is in $[-100, +100]$, and the resolution is one. Furthermore, the 1-dimensional case is considered where the arithmetic operations, on the elements of a high dimensional agent, are independent.

5.1. Sooty Tern Optimization Algorithm

The PDFs of the intermediate processing stages in STOA are depicted in Fig. 1. For the convergence to the best-so-far is illustrated in Eq. (4) and Fig. 1(a). In the case where $\mathbf{x}^*(t) - \mathbf{x}(t)$ falls within the range $[-1, +1]$, and is multiplied by \mathbf{r} in the interval $[0, 1]$, the product is less than both the multiplier and the multiplicand. As a result, a peak is observed in the PDF around zero.

In the exploitation stage, the PDFs of the $\sin(\theta)$ and $\cos(\theta)$ terms are shown in Fig. 1(b). Distinct peaks are observed at the angles 0 or 2π , $\pi/2$, π , and $3\pi/2$. In this plot, the angle resolution is 10^{-2} radians. The PDFs of α , β , γ , and ρ are presented in Fig. 1(c). As a correction is applied, the exponent term is bounded such that $\rho = \exp(-\theta) \in [0.0019, 1]$. Consequently, the PDFs are concentrated at small values compared to the range of the search space, which is $[-100, +100]$.

The update procedure described in Eq. (7) is illustrated by the PDF in Fig. 1(d). Since the update involves the multiplication of three components, the resulting PDF exhibits a peak around zero. This suggests that, due to the location of the agents, the algorithm tends to favor optima near zero. This behavior is undesirable, as for problems where the optimum is not near zero, the algorithm may fail to identify the correct optimum.

5.2. Tunicate Swarm Algorithm

The PDFs of the results obtained from the different computation stages in TSA are illustrated in Fig. 2. The PDF resulting from the computation of the movement factor, as described in Eq. (9), is shown in Fig. 2(a). A sharp peak is observed near zero. This is primarily due to the fact that the numerator, $4\mathbf{r}_3$, is larger than the denominator, $\mathbf{r}_1 + \mathbf{r}_2 - 2\mathbf{r}_3$, causing the quotient to become smaller. Additionally, since both the numerator and the denominator are positive, the quotient is also positive, and the PDF does not exist for negative values.

In the movement towards the best-so-far stage, the corresponding PDF is shown in Fig. 2(b). As before, due to the absolute value operation, the PDF only exists for positive values. Furthermore, the PDF decreases in a power-law manner at higher values.

The PDF of the remaining best-so-far stage is depicted in Fig. 2(c). The PDF takes on a triangular shape, with the maximum occurring at zero. The broader peak is the result of a simpler operation, which is merely the difference between a random number and the product of two other random numbers.

Regarding the swarm behavior stage, Fig. 2(d) illustrates the PDF. A narrow spike is observed around zero, which is caused by the division by a random number, $1 + \mathbf{r}_3 > 1$. Consequently, the triangular PDF observed in the remaining best-so-far stage is compressed. This phenomenon is undesirable in the search for the optimum.

5.3. Discussion

The PDFs of the final updated agent positions for both the STOA and TSA exhibit a pronounced peak around zero. This zero-bias phenomenon plays a crucial role in driving a significant portion of the results in each iteration toward zero. As a consequence, unless it is known in advance that the optimum lies near zero, these two algorithms are fundamentally limited in their ability to effectively and efficiently locate the optimum within the search space.

Furthermore, upon examining the computational procedures of these algorithms, it becomes evident that both multiplication and division operations involving random numbers are integral to their functioning. The former is clearly

observable in the STOA during the update stage, as presented in Eq. (7). The latter is likewise apparent in the TSA, specifically during the avoiding conflict stage (Eq. (8)) and the swarm behavior stage, see Eq. (11). In addition to these stages, the overall design of both algorithms incorporates various complex computational steps, the majority of which predominantly involve either multiplication or division. These two arithmetic operations, by their nature, contribute to a reduction in the probability of successfully locating the optimum, as they hinder the uniform distribution of agent positions across the search space. This lack of uniformity significantly impedes the exploration of the entire space, thereby limiting the algorithms' ability to find the true optimum.

In light of these observations, it is essential that future designs of BNIOAs give careful consideration to the simplification of the operations involved. Moreover, particular attention should be paid to ensuring that the issue of zero-bias can be effectively avoided, thereby enhancing the general applicability of this class of algorithms.

6. Conclusion

This paper provides a critical commentary on the STOA and TSA, directly addressing the theoretical underpinnings of the zero-bias phenomenon highlighted in (Kudela, 2022). Our analysis, grounded in probability theory, definitively confirms the presence of zero-bias in these algorithms. This is clearly demonstrated by the peaks observed in the PDFs during various computation stages, including the final update of agent positions. BNIOAs that exhibit this significant flaw are fundamentally unsuitable for optimization problems where the optimum is not located at zero. Therefore, any application of the STOA and TSA should be approached with full awareness of these critical limitations, which severely undermine their effectiveness in broader contexts.

References

- Dhiman, G., Kaur, A., 2019. STOA: A bio-inspired based optimization algorithm for industrial engineering problems. *Engineering Applications of Artificial Intelligence* 82, 148–174.
- Kaur, S., Awasthi, L.K., Sangal, A.L., Dhiman, G., 2020. Tunicate swarm algorithm: A new bio-inspired based metaheuristic paradigm for global optimization. *Engineering Applications of Artificial Intelligence* 90, 103541.
- Kudela, J., 2022. Commentary on: "STOA: A bio-inspired based optimization algorithm for industrial engineering problems "[EAAI, 82 (2019), 148–174] and "Tunicate swarm algorithm: A new bio-inspired based metaheuristic paradigm for global optimization"[EAAI, 90 (2020), no. 103541]. *Engineering Applications of Artificial Intelligence* 113, 104930.
- Sörensen, K., 2015. Metaheuristics—the metaphor exposed. *International Transactions in Operational Research* 22, 3–18.

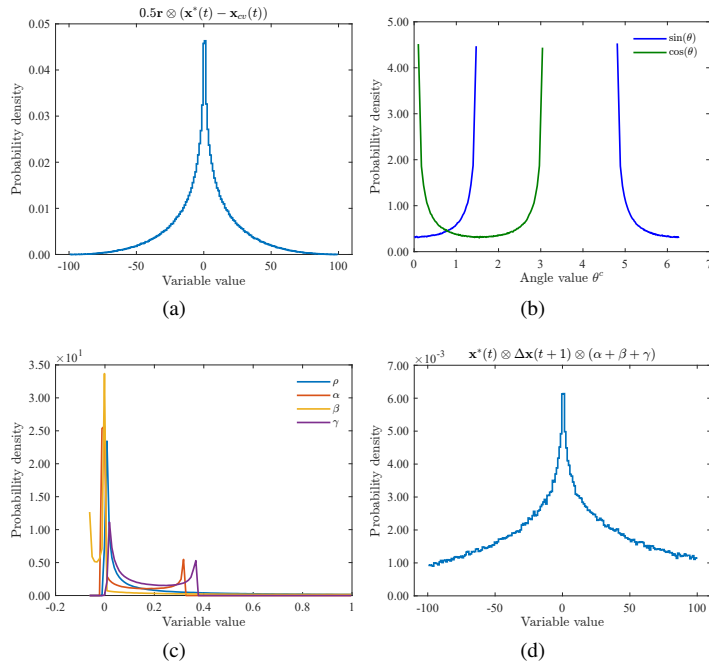


Figure 1: Probability density functions of the intermediate STOA stages. (a) convergence to best-so-far, (b)sine and cosin terms in Eq. (6), (c) exploitation stage, (d) updated agent position.

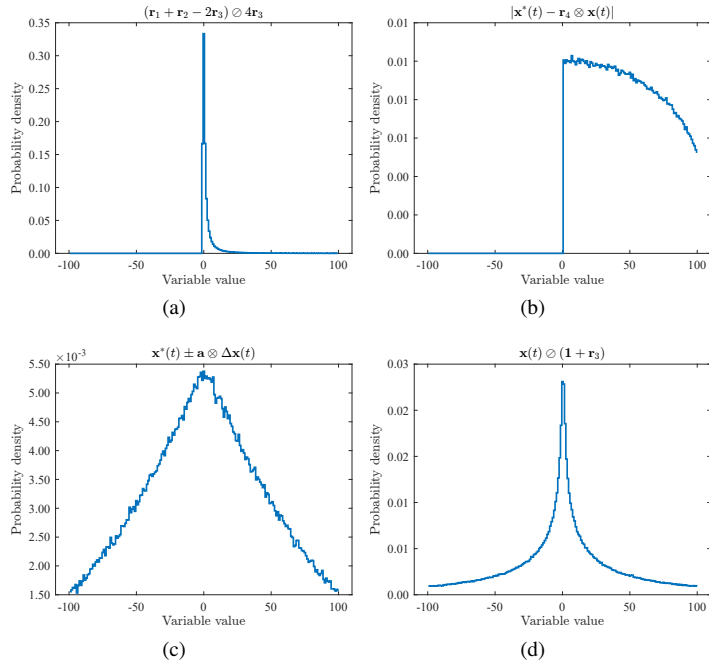


Figure 2: Probability density functions of the intermediate TSA stages. (a) movement factor \mathbf{a} , (b) movement towards best-so-far, (c) remain around best-so-far, (d) swarm behavior.